Non-distorting Flattening for Virtual Colonoscopy

Steven Haker[1], Sigurd Angenent[2], Allen Tannenbaum[3], and Ron Kikinis[4]

[1] Departments of Computer Science and Diagnostic Radiology,
Yale University, New Haven CT 06520.
haker@cs.yale.edu
[2] Department of Mathematics,
University of Wisconsin, Madison WI 53705.
[3] Departments of Electrical and Computer Engineering and Biomedical Engineering,
Georgia Institute of Technology, Atlanta GA 30332-0250.
tannenba@ece.gatech.edu
[4] Harvard Medical School, Brigham and Women's Hospital,
Harvard University, Boston MA 02115.

Abstract. In this paper, we consider a novel 3D visualization technique based on conformal surface flattening for virtual colonoscopy. Such visualization methods could be important in virtual colonoscopy since they have the potential for non-invasively determining the presence of polyps and other pathologies. Further, we demonstrate a method which presents a surface scan of the entire colon as a cine, and affords a viewer the opportunity to examine each point on the surface without distortion. From a triangulated surface representation of the colon, we indicate how the flattening procedure may be implemented using a finite element technique. We give a simple example of how the flattening map can be composed with other maps to enhance certain mapping properties. Finally, we show how the use of curvature based colorization and shading maps can be used to aid in the inspection process.

1 Introduction

Three dimensional visualization is becoming an increasingly important technique in surgical planning, non-invasive diagnosis and treatment, and image-guided surgery. Surface warping and flattening, which allow the easy visualization of highly undulated surfaces, are methods that are becoming increasingly widespread. For example, flattened representations of the brain cortical surface are essential in functional magnetic resonance imaging since one wants to show neural activity deep within the folds or sulci of the brain. 3D visualization is also of great importance in virtual colonoscopy in which one can non-invasively determine the presence of pathologies.

Virtual colonoscopy is currently an active area of research by radiologists as a minimally invasive screening method for the detection of small polyps (see [8] and the references therein). In the colon, this has become possible because of imaging devices which allow single breath hold acquisitions of the entire abdomen

at acceptable resolutions. Most reports have focused on methods which use computer graphics to simulate conventional colonoscopic procedures [8,13,14]. Virtual colonoscopy has some fundamental problems, which it shares with conventional colonoscopy. The most important one is that the navigation using inner views is very challenging and it happens frequently that sizable areas are not inspected at all, leading to incomplete examinations. An alternative approach for the inspection of the entire surface of the colon is to simulate the approach favored by pathologists, which involves cutting open the tube represented by the colon, and laying it out flat for a comprehensive inspection. In some recent work [11], a visualization technique is proposed using cylindrical and planar map projections. It is well-known that such projections can cause distortions in shape as is discussed in [11] and the references therein.

In this paper, we take another approach. We present a method for mapping the colon onto a flat surface in a conformal manner. A *conformal mapping* is a one-to-one mapping between surfaces which preserves angles, and thus preserves the local geometry as well. Our approach to flattening such a surface is based on a certain mathematical technique from Riemann surface theory, which allows us to map any highly undulating tubular surface without handles or self-intersections onto a planar rectangle in a conformal manner. There is some related work in the interesting paper [15] on the topological flattening of a tube onto the plane and its application to virtual colonoscopy. In [15], an electro-magnetic field is simulated by placing charges along a fly-through path. The resulting field lines which emanate from a point on the path define a surface whose intersection with the colon surface forms a loop which is flattened into the plane.

Our approach differs in that no flight path needs to be calculated, and the conformal nature of our flattening map allows us to enhance mapping properties and correct for distortion.

From a triangulated surface representation of the colon, we indicate how the flattening function may be found by solving a second order elliptic partial differential equation (PDE) using finite element techniques. Once the colon surface has been flattened onto a rectangular region of the plane, we utilize a method by which the entire colon is presented as a cine, and which allows the viewer to examine each surface point *without distortion* at some time in the image sequence. Thus in this sense 100% view with 0% distortion can be achieved. Moreover, we explicitly show how various structures of the colon may be studied using this approach. We demonstrate the use of shading maps and colorization as a function of surface curvatures to enhance visualization and inspection.

2   Analytical Approach to Colon Flattening

We first consider a mathematical model for the colon surface. See [3,6] for the full details. Let $\Sigma \subset \mathbf{R}^3$ represent a smooth embedded surface (no self-intersections) which is topologically an open-ended cylinder. The boundary of Σ consists of two topological circles, which we will call σ_0 and σ_1. We want to introduce a cut C on Σ from end to end, and construct an angle preserving one-to-one

map $f : \Sigma \backslash C \rightarrow \mathbf{R}^2$, which sends $\Sigma \backslash C$ to a rectangle R such that σ_0 and σ_1 are mapped to the left and right hand edges of R respectively, while the cut C is mapped to the upper and lower edges of R. The construction of f begins by finding, before the cut is made, a solution u to the Dirichlet problem $\Delta u = 0$ on $\Sigma \backslash (\sigma_0 \cup \sigma_1)$, with boundary conditions $u = 0$ on σ_0, and $u = 1$ on σ_1. Here Δ is the Laplace-Beltrami operator [12] on the surface Σ.

The cut C on Σ is then determined as the trace of the smooth curve obtained by following the gradient of u from a point on σ_0 to σ_1. We next compute the harmonic function v which is conjugate to u by specifying boundary conditions on the cut surface and again solving a Dirichlet problem; see [6]. The mapping $f = (u, v)$ sends the surface Σ to a rectangle R, as desired. The mapping can easily be extended across the cut and thus the cut need not hinder visualization.

3   Approximating the Flattening Function

In the previous section, we outlined the analytical procedure for finding the flattening map f. Here we will discuss the finite element method for finding an approximation to this mapping. See [9] for details about this method. In [1], we described a related method for brain flattening. However, because of the differences in topology between the brain and colon surface, the boundary conditions for the flattening maps are quite different. We now assume that Σ is a triangulated surface, and we look for a flattening map f which is continuous on Σ and linear on each triangle. Here, we will concentrate on finding u, the method for its conjugate v being similar.

It is a classical result [12] that the harmonic function u is the minimizer of the Dirichlet functional

$$\mathcal{D}(u) := \frac{1}{2} \int \int_{\Sigma} |\nabla u|^2 dS, \ \ u|_{\sigma_0} = 0, \ \ u|_{\sigma_1} = 1, \tag{1}$$

where ∇u is the gradient with respect to the induced metric on Σ. Let $PL(\Sigma)$ denote the space of piecewise linear functions on Σ. For each vertex $V \in \Sigma$, let ϕ_V be the continuous function, linear on each triangle, such that

$$\begin{aligned} \phi_V(V) &= 1, \\ \phi_V(W) &= 0, \ W \neq V. \end{aligned} \tag{2}$$

This set $\{\phi_V\}$ forms a basis for $PL(\Sigma)$, and so any $u \in PL(\Sigma)$ can be written as

$$u = \sum_{V \in \Sigma} u_V \ \phi_V. \tag{3}$$

To approximate the solution to the PDE, we minimize $\mathcal{D}(u)$ over all $u \in PL(\Sigma)$ which satisfy the boundary conditions. To minimize $\mathcal{D}(u)$, we introduce the matrix

$$D_{VW} = \int\int \nabla\phi_V \cdot \nabla\phi_W \ dS, \tag{4}$$

for each pair of vertices V, W. Since $D_{VW} \neq 0$ if and only if V, W are connected by some edge in the triangulation, D is sparse. Simple formulas exist [1,6,9] for the calculation of the elements of D; these formulas involve only the angles between adjacent surface edges. One can show that $u = \sum_V u_V \phi_V$ minimizes the Dirichlet functional over $PL(\Sigma)$ with the boundary conditions, if for each vertex $V \in \Sigma \backslash (\sigma_0 \cup \sigma_1)$,

$$\sum_{W \in \Sigma\backslash(\sigma_0\cup\sigma_1)} D_{VW}\, u_W = -\sum_{W\in\sigma_1} D_{VW}. \tag{5}$$

This is simply a matrix equation. One can quickly solve for the unknown $\{u_W\}$ using standard tools from linear algebra such as the conjugate gradient method.

4 Inspection and Distortion Removal

In practice, once the colon surface has been flattened into a rectangular shape, it will need to be visually inspected for various structures. In this section, we present a simple technique by which the entire colon surface can be presented to the viewer as a sequence of images or cine. In addition, this method allows the viewer to examine each surface point without distortion at some time in the cine. Here, we will say a mapping is without distortion at a point if it preserves the intrinsic distance there. It is well known that a surface can not in general be flattened onto the plane without some distortion somewhere [4]. However, it may be possible to achieve a surface flattening which is free of distortion along some curve. The Mercator projection of the earth does this along the equator. See [11] for a nice discussion of the classical geographic projections and their application to virtual colonoscopy. In our case, the distortion free curve will be a level set of the harmonic function u described above (essentially a loop around the tubular colon surface), and will correspond to the vertical line through the center of a frame in the cine. Specifically, suppose we have conformally flattened the colon surface onto a rectangle $R = [0, u_{max}] \times [-\pi, \pi]$. Let F be the inverse of this mapping, and let $\phi^2 = \phi^2(u, v)$ be the amount by which F scales a small area near (u, v), i.e. let $\phi > 0$ be the "conformal factor" for F. Fix $w > 0$, and for each $u_0 \in [0, u_{max}]$ define a subset $R_0 = ([u_0 - w, u_0 + w] \times [-\pi, \pi]) \cap R$ which will correspond to the contents of a cine frame. We define a mapping

$$(\hat{u}, \hat{v}) = G(u, v) = \left(\int_{u_0}^u \phi(\mu, v)d\mu, \int_0^v \phi(u_0, \nu)d\nu \right) \tag{6}$$

from R_0 to $\mathbf{C}$ which has differential

$$dG(u, v) = \begin{pmatrix} \hat{u}_u & \hat{u}_v \\ \hat{v}_u & \hat{v}_v \end{pmatrix} = \begin{pmatrix} \phi(u, v) & \int_{u_0}^u \phi_v(\mu, v)d\mu \\ 0 & \phi(u_0, v) \end{pmatrix} \tag{7}$$

and in particular $dG(u_0, v) = \phi(u_0, v) \times \begin{pmatrix} 1 & 0 \\ 0 & 1 \end{pmatrix}$. The conformality of the
flattening map, together with this value for $dG(u_0, v)$, implies that the composition of the flattening map with G sends the level set loop $\{u = u_0\}$ on the colon surface to the vertical line $\{\hat{u} = 0\}$ in the $\hat{u}$–$\hat{v}$ plane without distortion. In addition, it follows from the formula for dG that lengths measured in the $\hat{u}$ direction accurately reflect the lengths of corresponding curves on the colon surface.

5   Application

We tested our algorithms on $256 \times 256 \times 124$ CT colon data sets provided to us by the Surgical Planning Laboratory of Brigham and Women's Hospital. Two slices from one such data set are shown in Fig. 1. First, using the fast segmentation methods of [10] we found the colon surface. Unfortunately, the segmentation algorithm itself does not guarantee that the surface found will be a topological cylinder. In fact, it may contain numerous minute handles which arise because the boundary of the colon, as represented in the data set, may not be sharp. We used a morphological based method [7] by which these handles can be effectively removed and a surface which has the the topology of a closed-ended cylinder can be extracted. This is done in such a way that the large-scale geometry of the surface is not adversely affected.

Our segmentation method is a so called "level-set" method, in which the colon surface to extract is defined implicitly as the zero level set $\{(x, y, z) \mid \Psi(x, y, z) \equiv 0\}$ of a function Ψ defined on the 3D volume. It is well known that the Gaussian and mean curvatures of such an iso-surface can be calculated from the derivatives of Ψ; doing so allows us to avoid having to make these calculations on the triangulated surface after extraction. In fact, we may use the function Ψ to determine the entire second fundamental form for the iso-surface, using the formula

$$II = \frac{-1}{||\nabla \Psi||} T^{\,t} H_{\Psi} T \tag{8}$$

where H_{Ψ} is the 3×3 Hessian matrix of second derivatives of Ψ, and T is a 3×2 matrix whose columns are arbitrary orthonormal vectors perpendicular to the surface normal $N = \frac{\nabla \Psi}{||\nabla \Psi||}$. The eigenvectors e_1 and e_2 of II yield the principal directions (the directions in which the degree of surface bending is extremal) as Te_1 and Te_2, while the eigenvalues k_1, k_2 are the corresponding principal curvatures. See [5] for applications of principal direction vectors to surface visualization. The Gaussian curvature can then be found by $K = k_1 k_2 = Det(II)$, the mean curvature by $H = \frac{1}{2}(k_1 + k_2) = \frac{1}{2}Trace(II)$.

One would expect polyps to have relatively high Gaussian curvature as compared to the flatter surrounding colon surface. Further, these areas should be convex with respect to the colon interior, and thus have positive mean curvature

with respect to the outward surface normal. This suggests that for visualization, we color the flattened surface according to the Gaussian curvature of the colon surface, but only where both the Gaussian and mean curvatures of the colon surface are positive. The other areas may be colored with some neutral color. This alone, however, is not satisfactory for visualization of the flattened colon because the folds of the colon will not be represented. One solution to this problem is to use *shading maps*, an idea from computer graphics. The idea is to translate surface normals from the original surface to the corresponding point on the flattened surface. When rendered under identical lighting conditions, the original surface and the flattened surface with these "pseudo-normals" will have similar appearances, due to similar shading. This allows us to color the surface any way we wish, and still have the surface folds distinguishable in the flattened representation.

In Fig. 2, two views of the extracted colon surface and the corresponding flattened surface are shown using the coloring and shading scheme described above. We broke the flattened surface into two pieces to fit the page. The flattened surface is not exactly rectangular because we cut the colon surface along triangle edges rather than following the gradient of u exactly as described in Section 2. Fig. 3 shows more detailed views. On the left is an exterior view of a piece of the colon surface. In the center is a "fly-through" view of the same region, and on the right is the corresponding flattened region, corrected for distortion along the vertical center line as described in Section 4. In practice this image would be a single frame of a cine. Notice that the entire section of the colon is visible in the flattened version, while the coloring and shading scheme indicate the convex areas and surface folds. We are currently investigating the usefulness of this visualization scheme for the detection of polyps in a clinical setting.

The distortion correction method described in Section 4 is an example of how the conformal flattening map may be composed with another map to obtain desired mapping properties. Another simple example of this sort of enhancement is shown in Fig. 4. Here, we have composed the flattening map with another one-to-one conformal mapping from the plane to itself. This second conformal mapping was chosen to minimize the overall distortion of area in a least squares sense. However, it is not possible to correct for all distortion this way. Other such enhancing compositions are a current area of research [2].

References

1. S. Angenent, S. Haker, A. Tannenbaum, R. Kikinis, "Laplace-Beltrami operator and brain surface flattening," *IEEE Trans. Medical Imaging*, **18** (1999), pp. 700-711.
2. S. Angenent, S. Haker, A. Tannenbaum, R. Kikinis, "On area preserving mappings of minimal distortion," in *System Theory: Modeling, Analysis, and Control*, edited by T. Djaferis and I. Schick, Kluwer, Holland, 1999, pp. 275-287.
3. H. Farkas and I. Kra, *Riemann Surfaces*, Springer-Verlag, New York 1991.
4. M. P. Do Carmo, *Riemannian Geometry*, Prentice-Hall, Inc. New Jersey, 1992.

5. A. Girshick, V. Interrante, S. Haker, T. Lemoine. "Line direction matters: an argument for the use of principal directions in 3D line drawings," *First International Symposium on Non Photorealistic Animation and Rendering (NPAR 2000)*, to appear.

6. S. Haker, S. Angenent, A. Tannenbaum, R. Kikinis, "Nondistorting flattening maps and the 3D visualization of colon CT images," Technical Report, Department of Electrical Engineering, Georgia Tech, November 1999. Submitted for publication to *IEEE Trans. of Medical Imaging.*

7. S. Haker, "Extracting simply connected iso-surfaces from volumetric data," in preparation.

8. A. Hara, C. Johnson, J. Reed, R. Ehman, D. Ilstrup, "Colorectal polyp detection with CT colography: two- versus three-dimensional techniques," *Radiology* **200** (1996), pp. 49-54.

9. T. Hughes, *The Finite Element Method,* Prentice-Hall, New Jersey, 1987.

10. S. Kichenasamy, P. Olver, A. Tannenbaum, A. Yezzi, "Conformal curvature flows: from phase transitions to active contours," *Archive Rational Mechanics and Analysis* **134** (1996), pp. 275-301.

11. D. Paik, C. Beaulieu, R. Jeffrey, C. Karadi, and S. Napel, "Visualization modes for CT colonography using cylindrical and planar map projections," Technical Report, Department of Radiology, Stanford University School of Medicine, Stanford, CA, 1999.

12. J. Rauch, *Partial Differential Equations*, Springer-Verlag, New York 1991.

13. G. Rubin, S. Napel, and A. Leung, "Volumetric analysis of volumetric data: achieving a paradigm shift," *Radiology* **200** (1996), pp. 312-317.

14. D. Vining, "Virtual endoscopy: is it reality?," *Radiology* **200** (1996), pp. 30-31.

15. G. Wang, E. McFarland, B. Brown, and M. Vannier, "GI tract unraveling with curved cross sections," *IEEE Trans. Med. Imaging* **17** (1998), pp. 318-322.
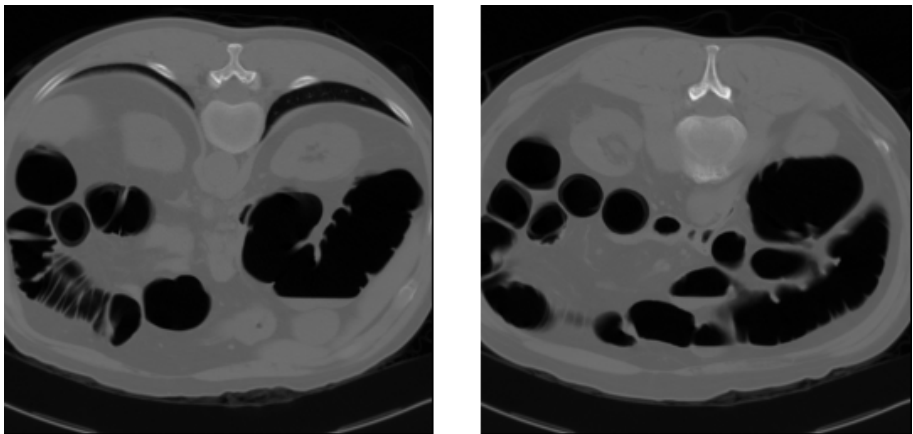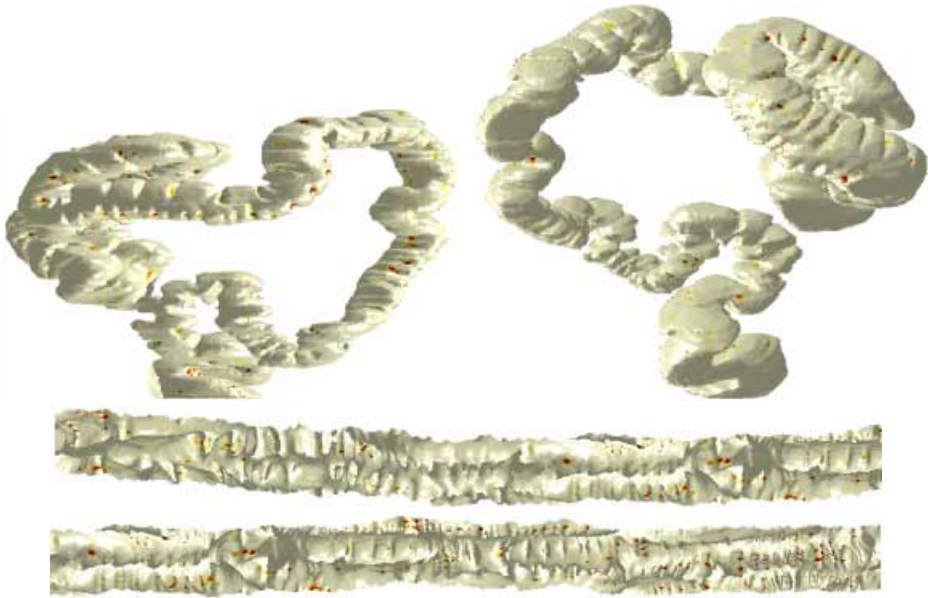
Fig. 1. Two Slices from CT Colon Data Set

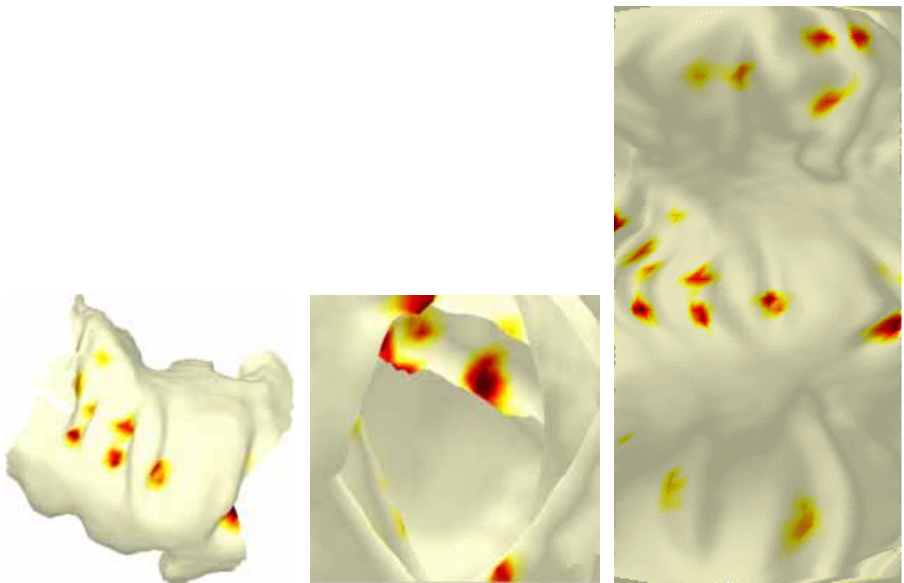**Fig. 2.** Two Views of Colon Surface and Flattened Representation

Fig. 3. Exterior, Fly-Through and Flattened Views

Fig. 4. Improved Conformal Mapping with Detail